China Ocean Eng., 2020, Vol. 34, No. 3, P. 341–351
DOI: https://doi.org/10.1007/s13344-020-0031-7, ISSN 0890-5487
http://www.chinaoceanengin.cn/ E-mail: coe@nhri.cn

Experimental Investigation of Disturbing the Flow Field on the Vortex-Induced Vibration of Deepwater Riser Fitted with Gas Jetting Active Vibration Suppression Device

LI Peng[a, b, *], JIANG Zhen-xing[a, b], LIU Yu[a, b], WANG Yu[a, b], GUO Hai-yan[c], WANG Fei[a, b], ZHANG Yong-bo[d]

[a] College of Civil Engineering and Architecture, Shandong University of Science and Technology, Qingdao 266590, China

[b] Shandong Provincial Key Laboratory of Civil Engineering Disaster Prevention and Mitigation, Qingdao 266590, China

[c] College of Engineering, Ocean University of China, Qingdao 266100, China

[d] National Oceanographic Center of Qingdao, Qingdao 266071, China

Received August 1, 2019; revised December 13, 2019; accepted January 10, 2020

Abstract

An experimental investigation on the disturbance effect of jet-type active vibration suppression device on vortex-induced vibration of deep-sea riser was carried out in the wave-flow combined flume. The vibration suppression device was designed in which the jet pipe was horizontally fixed to the front end of the riser. By varying three different excitation spacings and multi-stage outflow velocities, the influence law of the dominant frequency, dimensionless displacement and other dynamic response parameters was studied under different excitation spacings, and the mechanism and sensitive characteristics of the disturbance suppression were explored. The results indicate that the variation of excitation spacing makes gas curtain enter the strong disturbed flow region at different velocities and angles, and the coupling relationship between excitation spacing and reduced velocity is the key factor to enter the strong disturbed flow region to achieve the optimal disturbance suppression. In the strong disturbed flow region, the influence of gas curtain on the dominant frequency is obviously affected by the flow velocity, while the vibration displacement is stable at the same amplitude and is weakly affected by the flow velocity. Gas curtain can effectively disturb the formation of vortex shedding, destroy the strong nonlinear coupled vibration of the riser, and achieve better vibration suppression effect. In the weak disturbed flow region, the vortex length of the riser tail is prolonged, the strong nonlinear coupled vibration of the riser is gradually restored, and the vibration suppression effect of the device gradually decreases.

Key words: deepwater riser, vortex-induced vibration (VIV), active vibration suppression, jet-type, excitation spacing, disturbance flow

Citation: Li, P., Jiang, Z. X., Liu, Y., Wang, Y., Guo, H. Y., Wang, F., Zhang, Y. B., 2020. Experimental investigation of disturbing the flow field on the vortex-induced vibration of deepwater riser fitted with gas jetting active vibration suppression device. China Ocean Eng., 34(3): 341–351, doi: https://doi.org/10.1007/s13344-020-0031-7

1 Introduction

Riser systems, known as the drill conductor systems linking surface floating bodies to seabed wellheads, are the basic installations for a floating production system to deliver liquids to ships, as well as the most complicated part of a deepwater production system. They can be devided into steel catenary risers (SCRs), top tension risers (TTRs), flexible risers, and hybrid risers, according to structural type. Given the large aspect ratios of these structures and their constant exposure to complicated marine loads such as waves and ocean currents, vortex-induced vibration (VIV) constitutes the main driver for their fatigue damage (Baarholm et al., 2006; Wang et al., 2013, 2014; Gao et al., 2016, 2017; Chaplin et al., 2005; Song et al., 2016).

In order to effectively minimize riser damages caused by VIV, many authors have experimentally investigated how VIV can be suppressed. They suggested that this can be achieved by either changing the properties of the structure

Foundation item: This work was supported by National Natural Science Foundation of China (Grant No. 51709161), the Key Research and Development Program of Shandong Province (Grant Nos. 2019GHY112061 and 2018GHY115045), Research and Innovation Team of Ocean Oil and Gas Development Engineering Structure, College of Civil Engineering and Architecture, Shandong University of Science and Technology (Grant No. 2019TJKYTD01). Shandong Provincial Natural Science Foundation, China (Grant No. ZR2017BEE041). Science and technology innovation project for postgraduates of Shandong University of Science and Technology (Grant No. SDKDYC180327).

*Corresponding author. E-mail: lipeng@sdust.edu.cn

itself or installing a vibration suppression device. Overall, two ways are available to suppress VIV of the riser. One is called passive suppression, which prevents the formation of vortexes by changing the surface geometry of the structure or adding other devices on the surface of the structure. Many scholars have measured the dynamic response of the vibration suppression riser under different working conditions by dragging or manufacturing the outflow. More classically, Trim et al. (2005) studied the vibration suppression effect of the vortex-induced vibration of the riser under the action of uniform flow by dragging a 38-meter-long horizontally placed riser model and using the two coverage rates of the triple helical strakes. Meanwhile, many other types of passive vibration suppression devices have emerged. For instance, Huera-Huarte (2014) proposed to use a splitter plate elastically installed on the surface of a flexible riser to suppress vortex-induced vibration. Cicolin and Assi (2017) designed a flexible sheath to carry out vibration suppression tests on low-mass and low-damping cylinders. At present, passive vibration suppression devices have made many achievements in theoretical and experimental researches, as widely used in practical engineering. The other is called active suppression which actively disturbs the flow field in the proximity of the riser and suppresses VIV with a driving device through external energy inputs such as acoustic waves, vibration or ejection and through real-time monitoring of ocean current variations. Its mechanism of action is to achieve VIV vibration suppression by changing the vortex shedding frequency deviating from the natural frequency of the structure and changing the wake of the body, to achieve more self-applicable and effective control. In recent years, many scholars have also studied active vibration suppression devices, mainly from two directions: the actuator direction and the wake control direction. Warui and Fujisawa (1996) installed electromagnetic actuators at both ends of a cylinder to generate lateral vibration, thus causing changes in the near wake and reducing the formation of vortex shedding; Cheng et al. (2003) proposed a method of installing three piezoelectric ceramic actuators on the surface of a square cylinder to locally disturb the surface of a non-fluid body, and studied the interaction between synchronous cylinder motion and vortex shedding. Muddada and Patnaik (2010) directly input energy through an external source driven actuator to effectively control the wake of a cylinder. As to the wake control direction, Williams et al. (1992) and Williams and Zhao (1992) observed that the airflow ejected from the small holes on the cylinder surface significantly changed the flow wake behind the cylinder, thus achieving the purpose of suppressing vortex-induced vibration. Dong et al. (2008) proposed a new technology to eliminate the Karman vortex street formed in the wake of the cylinder, in which a steady suction is applied on the wind-ward half of the cylinder surface while a steady blowing is applied on the leeward half of the surface and so as to restrain the vibration of blunt body. Feng and Wang (2014) formed an envelope upstream of the cylinder through synthetic jet, causing wake changes, thus obtaining different control effects. Wang et al. (2017) conducted a numerical investigation of active VIV control of a cylinder using a pair of synthetic jets (SJs) at a low Reynolds number of 100. The SJ pair operates with various phase differences over a wide frequency range so that the influence of various lock-on can be investigated. It is found that the VIV control can be affected not only by the occurrence of the primary lock-on but also by the occurrence of other lock-on such as secondary and tertiary lock-on. Muddada and Patnaik (2017) proposed a simple active flow control strategy based on momentum injection to suppress vortex-induced vibration at low Reynolds numbers. The two small control cylinders located 120° behind the cylinder act as actuators, performing the required momentum injection to achieve the vibration suppression effect. Zhu et al. (2019) proposed a kind of gas jet vibration suppression device located on the shoulder of the riser, which can prevent the development of boundary layer and vortex shedding by injecting gas to achieve the purpose of vibration suppression. In summary, scholars from various countries have made much progress in active vibration suppression devices, but their test systems are still incomplete with bottleneck in the suppression effect, and the influence parameters and mechanism of the disturbance vibration suppression are not clear.

In this paper, the jet-type active vibration suppression device and its test system are designed. By changing the outflow velocity and excitation spacing, the influence law of the dynamic response of the jet active vibration suppression device on the dynamic response of the riser is studied from the determination of the vibration locking interval of the riser, the dominant frequency, the displacement response and the in-line (IL)—cross-flow (CF) coupling vibration to explore the disturbance suppression mechanism and sensitive characteristics of jet active vibration suppression device. Results of this paper can provide reference and scientific basis for the design and engineering application of active vibration suppression technology in riser.

2 Experimental layout

2.1 Supporting structure

The experiment was carried out in the wave-flow combined flume of the Engineering Hydrodynamics Laboratory, Ocean University of China. The flume measures 30.0 m (L) by 1.0 m (W) by 1.2 m (H), with the maximum velocity of 1.0 m/s, maximum wave height of 0.3 m and maximum working water depth of 1.0 m. The flume is sided with toughened glass, partitioned with steel columns and bottomed with steel plate which can be used for fixing the support of the riser. The entire system can be used to simulate regular waves and steady flow velocities and is therefore

suitable for our experiment.

As planned, we designed and fabricated a supporting device qualified for our experiment as a supporting structure to fix the test riser in the flume and apply initial tension to the riser. The 3.00 m×0.98 m×2.92 m supporting device was an assembly of 40 mm×40 mm and 40 mm×80 mm profiles. To ensure the stability of the supporting structure when exposed to flows, a Z-shaped fixing device was attached to a high-tensile bolt previously welded on the bottom of the flume, and the upper side ends of the structure were secured with G clamps. After the supporting structure had been assembled, its bearing capacity was checked and its stability was tested. The riser remained in a standing posture throughout the test, with its lower part (40%) immersed in a uniform flow field. Fig. 1 shows the overall layout of the experiment.

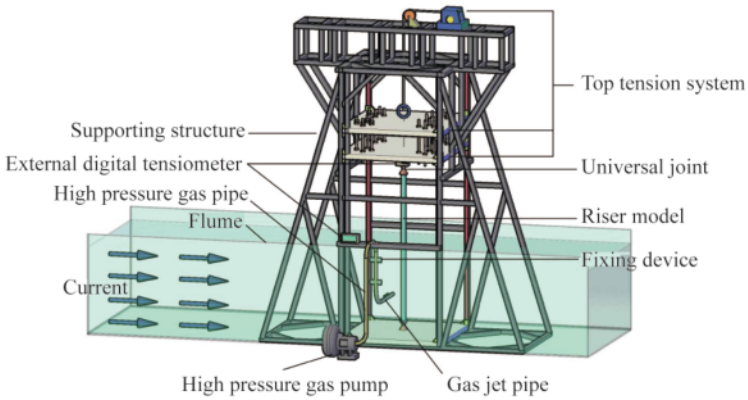

Fig. 1. Overall layout of the experiment.

In order to effectively fix the riser and compensate for the tension loss, this experiment used a top tension of 19.6 N. And for the accurate application of the top tension of the riser, a set of top tension application system adapted to the support structure is designed. It consists of a self-locking winch, a pulley, a perforated aluminum alloy plate, an external digital tensiometer, an SBR aluminum-supported linear guide, and a universal joint. By adjusting the winch, the desired amount of top tension could be applied to the riser. When the reading on the external digital tensiometer had reached the design value, the winch was automatically locked, locking the lead screw connecting the riser model onto the aluminum plate.

As the riser model was vertically stood inside the flume, to minimize its departure from the predesigned position, the riser was multi-dimensionally positioned with the help of professionals and an infrared positioner during installation to ensure that it was perpendicular to the inflow all the time.

2.2 Riser model and testing method

To present the vibration behavior of the riser under uniform inflows and investigate the sensitivity parameters and suppression pattern of the jet-type active vibration suppression device, a number of tubes were selected and tested for mechanical properties before a 2 m long organic glass tube was eventually used as the riser model. The risers were customized at a tube manufacturer and sampled for a number of times to ensure consistent mechanical properties among different riser models. The universal joint connecting the upper and lower ends of the riser model was fabricated by a machining workshop according to the design plan with a specifically designed machine tool. Fig. 2 and Table 1 show the positioning of the test riser and its detailed parameters.

During the experiment, an FBG strainometer and a SM130 demodulator (Micron Optics) were used to acquire data. Six locations were selected across the height of the riser as signal acquisition points. To ensure stable data sampling, data were sampled at a time interval of 40 s at each level after the external flow became stable. Four FBG strain sensors were mounted at each location at an angle of 90° to measure the CF and IL dynamic strains, as shown in Fig. 2.

2.3 Designing the jet-type active vibration supporting device

The jet-type active vibration suppression device was composed of a gas jet pipe, high-pressure gas pipes, metal connectors, a high-pressure gas pump, and an FBG sensor. The high-pressure gas pipes were connected to the gas jet pipe with metal connectors and fixed in parallel at the front of the riser, with the blowholes all pointing upward. Fig. 3 shows the design principle, excitation spacing, and real photo of the device. Three excitation spacings, namely, S = 10D, 15D and 30D (where S is the excitation spacing and D is the diameter of the riser) were used. In the remainder of this paper, the time before the initiation of the jet-type active vibration suppression device is called “before excitation” or “pre-excitation” and that after its initiation is called “after excitation” or “post-excitation”.

The gas curtain formation area and vertical inclination angle are significantly different under different outflow velocities with different excitation spacings. Therefore, the coupling effect of excitation spacing and outflow velocity

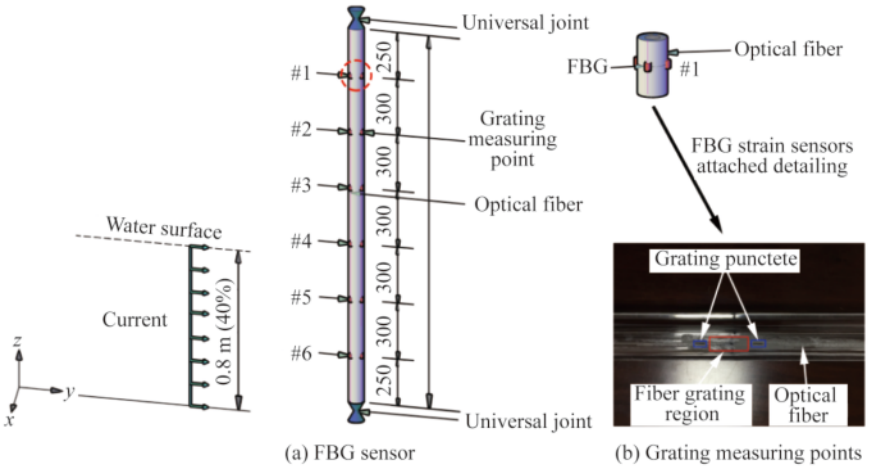

Fig. 2. Position of the surface FBG sensor of the test riser model: FBG sensor (a); grating measuring points (b).

Table 1 Geometric and mechanical parameters of the riser model

Parameter	Value	Unit
Riser model length L	2.00	m
Length of still water L_1	0.80	m
External diameter D	0.018	m
Thickness δ	0.001	m
Mass per unit length of riser m	0.065	kg/m
Aspect ratio L/D	111.11	--
Bending stiffness EI	4.63	Nm^2
Natural frequency f_1	3.30	Hz

on vibration suppression optimization results shows that the main body of the gas curtain formation area is located in the vortex street area behind the riser. And in this range, it is called a strong disturbed flow region, which can effectively destroy the periodic vortex shedding and achieve the purpose of disturbance and vibration suppression. When the main body of the gas curtain formation area leaves the vortex street area, its influence on vortex shedding is weakened, and its vibration suppression effect significantly decreases, which is called the weak disturbed flow region. The velocity and spacing are shown in Table 2.

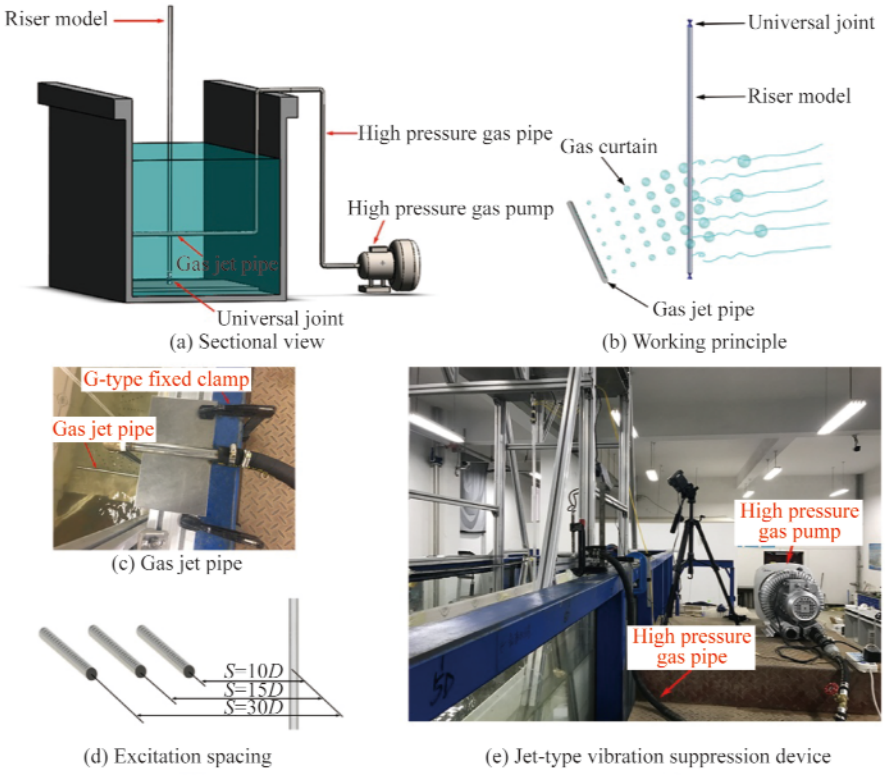

Fig. 3. Schematic of the design principle of the jet-type active vibration suppression device.

Table 2 Design working condition parameters

Case No.	Model type	Excitation spacing S	Velocity (m/s)
1	Riser before excitation	--	0.1–0.6
2	Riser after excitation	10D	0.1–0.6
3		15D	0.1–0.6
4		30D	0.1–0.6

Inspired by the existing literature and combined with the research contents and characteristics of this study, the detailed parameters of the designed gas jet pipe are as follows: pipe length 900 mm, diameter 20 mm, wall thickness 1 mm, pipe body evenly open three holes at 120°, aperture 2 mm, interval of each hole 20 mm, as shown in Fig. 4.

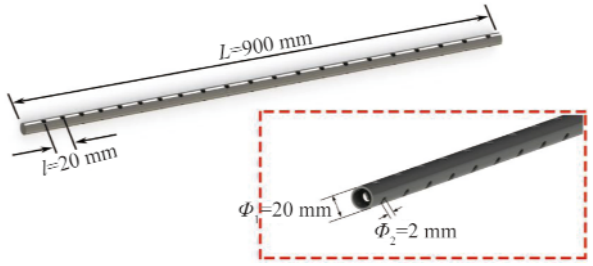

Fig. 4. Details of jet pipe.

The high-pressure gas pipes were connected to the high-pressure gas pump at the top and to the gas jet pipe at the bottom. When the external flow passed through the riser, high-pressure gas current was ejected through the gas jet pipe at the bottom. The gas current formed gas curtains at the sides of the riser. Fig. 5 shows the working scene of the jet-type active vibration suppression device.

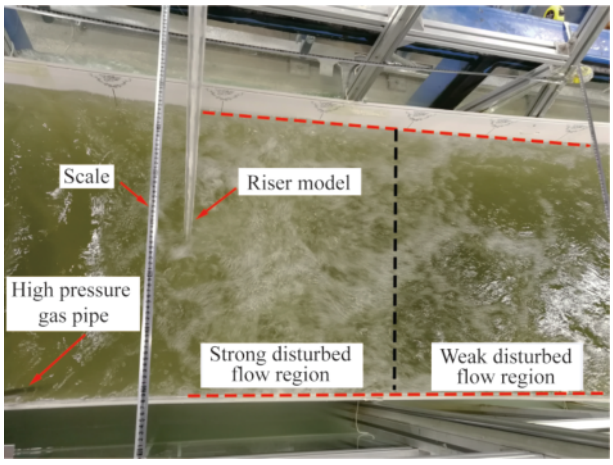

Fig. 5. Disturbed flow produced by the gas current.

3 Results and discussion

3.1 Frequency variation along reduced velocity

Fig. 6 shows the power spectral density along the reduced velocity in the CF direction of the riser before and after excitation, where f_s is the vortex shedding frequency and f_1 is the first-order natural frequency of the riser. It can be seen from Fig. 6 that when the active vibration suppression device is not started, the riser has a dominant frequency, and the vortex-induced vibration energy is concentrated at a single frequency peak, and follows Strouhal's law. When the device is started, the normal flow field is disturbed, and the dominant frequency of the riser is not obvious, because the gas curtain action position at each excitation spacing is in front of the riser when $Ur \leqslant 4.20$.

When S=10D, the riser is within the range of $4.20 \leqslant Ur \leqslant 5.05$, the rising gas curtain flow mixed with the incoming flow forms two opposite circulation flows on both sides of the gas curtain (Liu, 2010) due to the restriction of the free surface. Thus, the horizontal flow forms at a certain depth of the liquid surface. When the reduced velocity is small, the vortex shedding frequency of the riser is low, and the reverse horizontal flow damages the formation and development of the boundary layer of the riser, hinders its normal vortex discharge, attenuates the vortex-induced vibration energy, reduces the amplitude of power spectral density by an order of magnitude, and the dominant frequency is no longer obvious. With the increase of the reduced velocity, the vortex shedding frequency of the riser gradually becomes dominant when the gas curtain moves to the weak disturbed flow region. When the gas curtain passes through the riser, the bubbles inject momentum into the shear layer and boundary layer, causing the vortex formation length to be elongated (Zhu et al., 2019), resulting in the reduction of the dominant vibration frequency and vibration energy of the riser, but it still has obvious dominant frequency. The vibration frequency change trend of riser at S=15D is like that at S=10D, except that the strong disturbed flow region is $5.05 \leqslant Ur \leqslant 6.73$. However, when S = 30D, the gas curtain still has obvious influence on the dominant frequency of the opposition tube when $Ur \leqslant 5.05$. With the increase of the reduced velocity, vortex shedding frequency gradually regains the dominant position. When $Ur \geqslant 7.58$, the action position of the gas curtain is in the strong disturbed flow region when S=30D, the amplitude of the power spectral density of the riser vibration decreases greatly, and the dominant frequency is no longer obvious.

Based on the above description, it can be found that the coupling effect of flow velocity and gas curtain action position is the key to affect the dominant frequency of riser. When the gas curtain acts on the strong disturbed flow region, the dominant frequency of the riser is not obvious and the vortex-induced vibration energy decays. When the gas curtain acts on the weak disturbed flow region, the riser recovers its obviously dominant frequency and the vibration energy of the riser decreases.

3.2 Strain and displacement amplitudes

Fig. 7 is the strain–time histories at Ur=3.36, 5.89 and 10.10 before and after excitation at spacings in the CF direction. Figure analysis shows that, when Ur=3.36, due to the

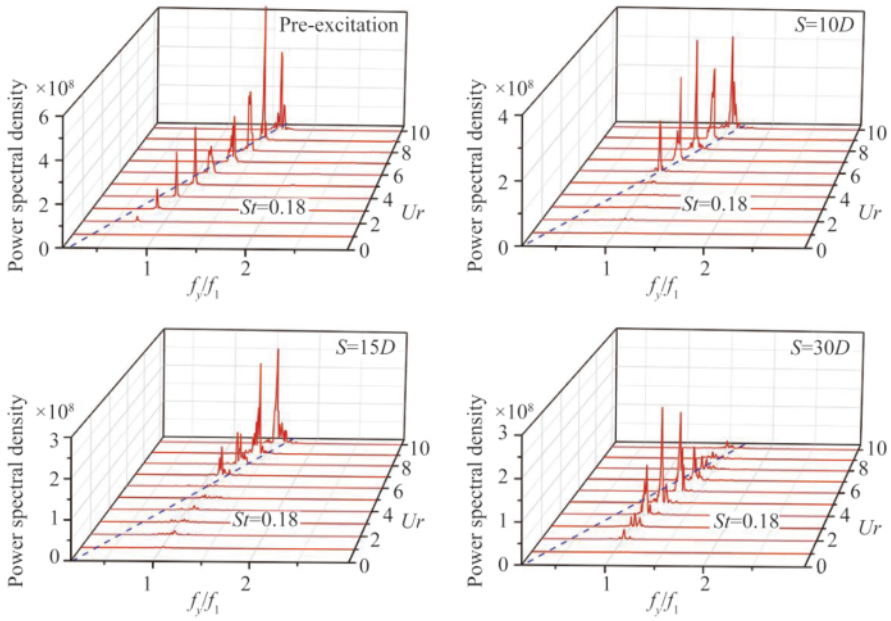

Fig. 6. Power spectral density along the reduced velocity in the CF direction of the riser before and after excitation.

existence of gas curtain, the normal vortex-induced vibration of the riser in water is destroyed, and the vibration strain-time history curves of the riser at various excitation spacings do not show a stable and symmetrical distribution similar to that before excitation. In addition, the strain was disordered and increased in the scope of oscilloscope. The primary reason is that the reduced velocity is low and the vortex-induced vibration amplitude of the riser is small. When S=10D and 15D, the gas curtain is located near the riser, the bubbles burst on the water surface and fluctuate on the water surface. The sawtooth fluctuation in the red line frame in the figure is an obvious sign of the influence of waves on the riser, which leads to drastic changes in the strain amplitude of the riser. While S=30D, the gas curtain action position is located far from the riser due to the long excitation spacing. Both the disturbance of bubble convection field and the circulation generated by ascending gas curtain flow affect the riser vibration, and the strain change is relatively gentle compared with the first two spacings. When Ur=5.89, S=10D and 15D, the gas curtain reaches the tail of the riser, and its strain also sawtooth fluctuates. In addition, the reverse circulation flow destroys the formation and development of the boundary layer behind the separation point, and the negative pressure gradient cannot be formed, which affects the formation of the reverse pressure region behind the riser. As a result, the downstream fluid cannot be separated at the separation point. Moreover, due to the nonuniformity of bubble rupture, its strain change is not uniform, and the overall strain amplitude becomes smaller. The strain amplitude of S=30D is like that of pre-excitation. As the gas curtain does not reach the tail of the riser, it only affects the flow field in front of the riser and the strain is relatively disordered. When Ur=10.10, the strain of S=10D and 15D becomes more stable at lower flow velocities, the periodic vibration is resumed, and the strain amplitude decreases slightly, the strain change period T increases slightly compared with that of pre-excitation. This is mainly due to the bubble injecting momentum into boundary layer and shear layer when the gas curtain passes through the riser, prolonging the vortex shedding period, causing the riser amplitude to decrease slightly. Nevertheless, the strain amplitude of S=30D is significantly different from that before excitation, and sawtooth fluctuation also occurs, but the tooth pitch is larger. At the same reduced velocity, the strain value is much lower than that with other excitation spacings. This means that at high reduced velocity, the vortex-induced vibration of the riser can still be obviously affected when the gas curtain is in strong turbulence region.

As an important parameter for the vibration amplitude of the riser, the displacement root mean square (RMS) can indicate how the riser vibrates within the sampling time. Based on the mode superposition method, the displacement RMS values of the riser at different measuring points have been calculated. Fig. 8 shows the dimensionless displacement RMS values of the riser in the CF direction under different reduced velocity. With the condition of $Ur \leqslant 3.36$, the three excitation spacings of the jet-type active vibration suppression device all intensify the riser vibration. As a result of the near excitation spacings and low reduced velocity, the bubbles generated by the active vibration suppression device at S=10D and S=15D burst near the riser, causing its forced vibration. However, when S=30D, the gas curtain acts on the front of the riser, and generates a turbulent flow

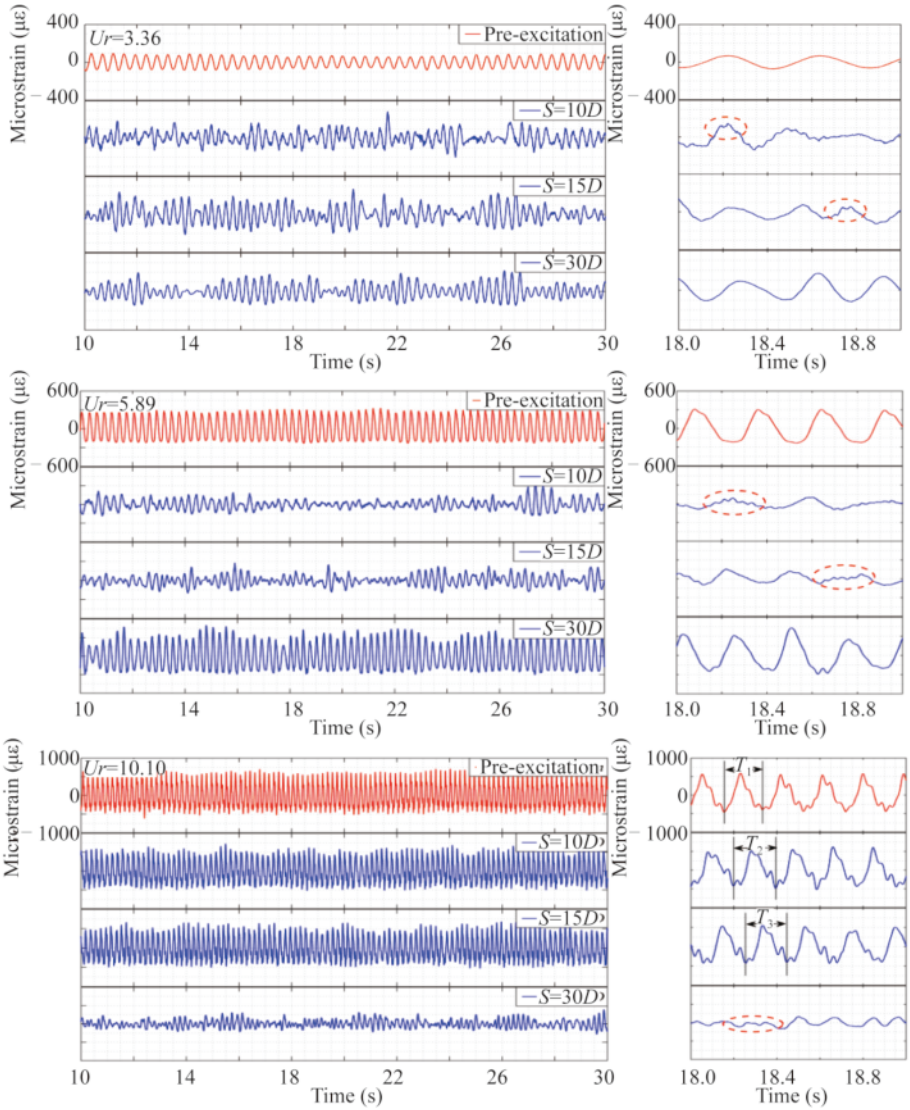

Fig. 7. Strain–time histories at Ur = 3.36, 5.89 and 10.10 before excitation and after excitation at different spacings in the CF direction.

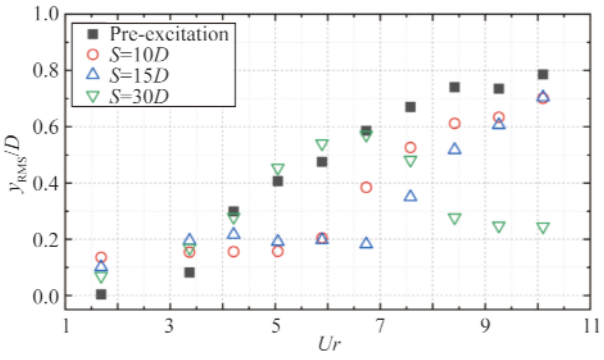

Fig. 8. Dimensionless displacement RMS values in the CF direction along the reduced velocity at different excitation spacings.

field and a positive horizontal flow, resulting in an increase in the displacement amplitude of the riser. With the further increase of the reduced velocity, the gas curtain generated by the active vibration suppression device at S=10D and S=15D enters the strong disturbed flow region within 4.20⩽Ur⩽5.89 and 5.05⩽Ur⩽6.73, respectively, and its dimensionless RMS displacement amplitude in the corresponding reduced velocity interval is stable around 0.20D, indicating that the two intervals achieved the same effect of vibration suppression. After that, the gas curtain enters the weak disturbed flow region with the reduced velocity and the dimensionless RMS displacement amplitude of riser shows an upward trend under the two excitation spacings after excitation. With the extension of the vortex shedding period, the RMS displacement is still smaller than that before the excitation. In addition, when S=30D, in the interval of 4.20⩽Ur⩽7.58, the RMS displacement of the riser increases, which is caused by the movement of the gas curtain action position; and then it enters the strong disturbed flow region when 8.42⩽Ur⩽10.10, and remains stable at around 0.25D. In summary, the gas curtain generated by each excitation spacings sequentially enters the strong dis-

turbed flow region along with the reduced velocity, and the rising gas curtain flow and the reverse horizontal flow effectively hinder the development of boundary layer and shear layer. The vibration displacement in the strong disturbed flow region is weakly affected by the flow velocity, thus achieving the purpose of disturbance and vibration suppression. After entering the weak disturbed flow region, the bubbles passing through the riser inject momentum into the boundary layer and shear layer, the vortex shedding period is prolonged, and the vibration displacement decreases slightly.

Fig. 9 shows displacement RMS values of the riser in the IL direction changes with the function of reduced velocity, the variation law is like that in the CF direction of the riser. The reduced velocity interval with stable amplitude of each excitation spacing after excitation is approximately the same as that in the CF direction. However, because the direction of horizontal flow is the same as that of the IL direction, and the decrease of displacement in the IL direction is larger than that in CF direction, the effect of reverse horizontal flow is more obvious in IL direction. Among them, when Ur=4.20, the riser vibration of S=10D and S=15D starts to stabilize. At high reduced velocity, the vortex-induced vibration of the riser with S=30D is intense. After the gas curtain enters the strong disturbed flow region, the RMS displacement of the riser is greatly reduced, and the displacement is reduced to the same as that of other excitation spacings in the strong disturbed flow region, which means that the displacement does not change with the reduced velocity when the gas curtain is in the strong disturbed flow region.

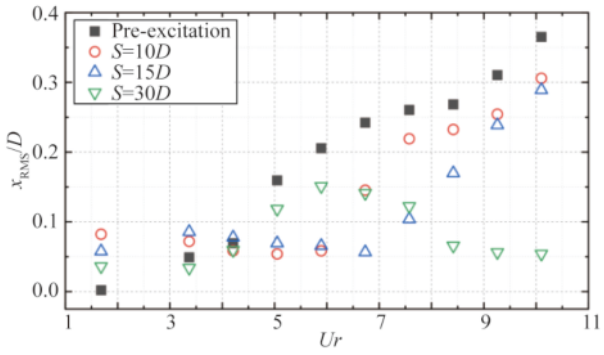

Fig. 9. Dimensionless displacement RMS values in the IL direction along reduced velocity at different excitation spacings.

Fig. 10 shows the modal weight changes and displacement envelope diagrams of S=10D, 15D and 30D when Ur=5.05, 6.73 and 10.10, respectively. Meanwhile, the modal weight and displacement envelope diagrams of the riser before excitation with the reduced velocity are also given for comparison. It can be clearly observed that the first two modes of the riser before the excitation contribute significantly and the dominant mode maintains regular and stable amplitude throughout the sampling process. In addition, with the increase of reduced velocity, the second-order modal weight of the riser before excitation increases gradually and its displacement envelope diagram also shows the same phenomenon. However, after starting the active vibration suppression device of gas injection, only the first-order mode dominates the riser, the weight of the second-order mode is not stable, and the spatial distribution is unstable and asymmetric. This is mainly due to the complex influence of the rising gas curtain flow on the wake of the riser, which can greatly change the additional mass distribution around the riser, and then change the modal response of the riser, so as to achieve the purpose of suppressing the vortex-induced vibration of the riser.

3.3 Suppression efficiency variation versus reduced velocity

Fig. 11 shows the suppression efficiencies of the jet-type active vibration suppression device in the CF direction as a function of different excitation spacings. As under a low reduced velocity, the gas curtain impact on the riser intensifies its vibration and all suppression efficiencies are negative, so the starting reduced velocity is Ur = 4.20 in this chart. In the S=10D and 15D states, the gas curtain respectively enters the strong disturbed flow region at 4.20$\leqslant Ur \leqslant$ 5.89 (range I) and 5.05$\leqslant Ur \leqslant$6.73 (range II), and the rising gas curtain flow interrupts the vortex street at the tail of the riser, and the circulation hinders the development of the boundary layer. As the reduced velocity increases, the gas curtain enters the weak disturbed flow region. The vibration suppression efficiency begins to decrease gradually, and the vibration suppression effect is no longer obvious, and finally the vibration suppression efficiency drops to about 10%. In the state of S=30D, the vibration suppression efficiency starts to decrease when Ur=4.20, which is due to the increase of the vibration of the riser caused by the change of the influence mode of the gas curtain on the riser. With the further increase of the reduced velocity, the position of the gas curtain gradually moves from the vicinity of the riser to the strong disturbed flow region at the rear of the riser, and the vibration suppression efficiency gradually increases. After Ur=8.42 (range III), the vibration suppression efficiency is stabilized at about 65%, and it still has a slight upward trend, finally reaching 67.6%. This means that when the active vibration suppression device acts in the strong disturbed flow region, the vibration suppression efficiency increases with the reduced velocity, but the increase is small, which is consistent with the phenomenon observed in Fig. 8.

The vibration suppression efficiency in the IL direction of the riser with the changes of the reduced velocity is shown in Fig. 12. The vibration suppression efficiency of the active vibration suppression device in the IL direction is almost the same as that in the CF direction. As the circula-

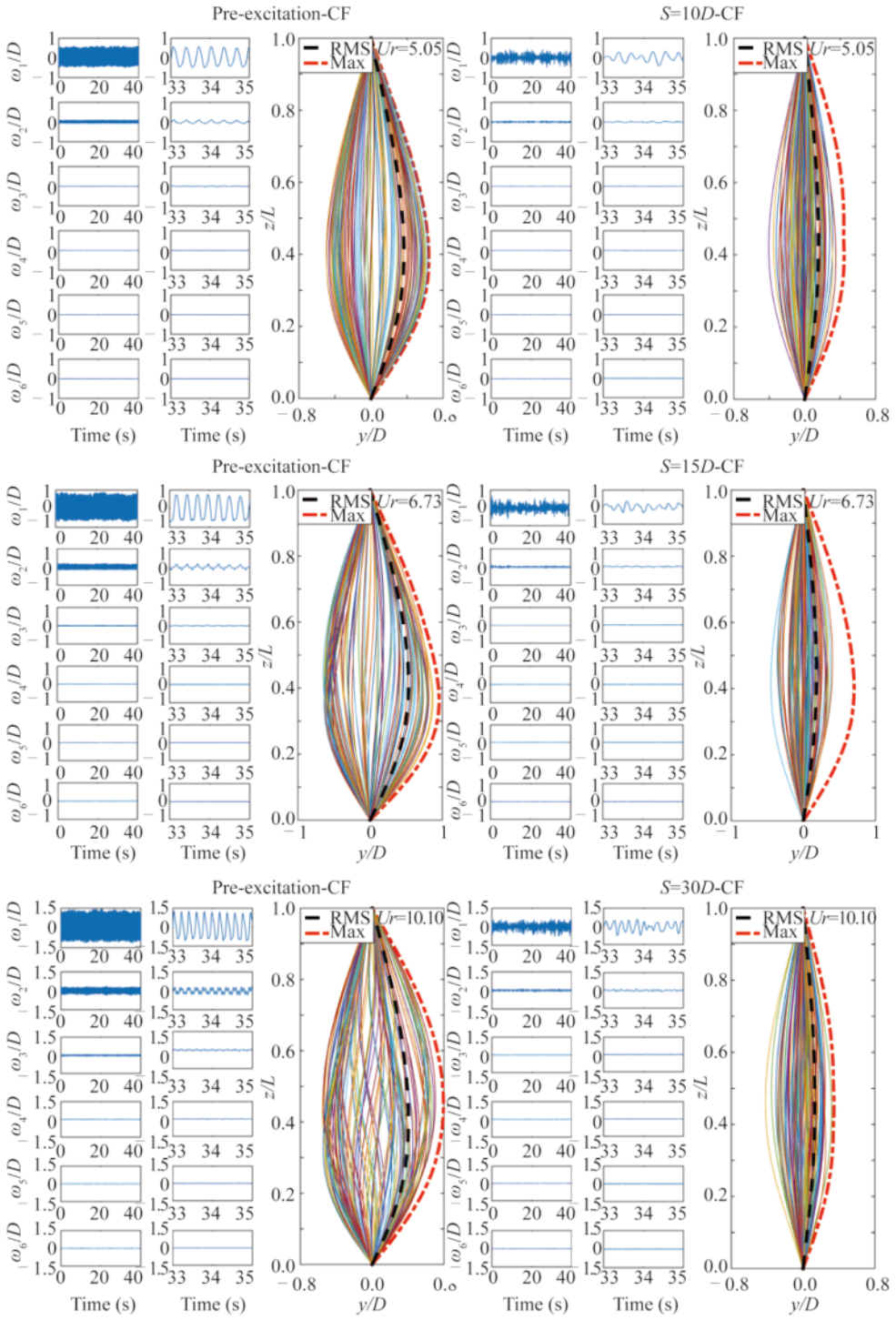

Fig. 10. Modal weight and displacement envelope of the riser before excitation at the same reduced velocity and the riser when the gas curtain action position is in the strong disturbed flow region.

tion flow direction generated by the gas curtain is the same as that of IL, the vibration suppression efficiency of the riser in IL direction is significantly higher than that in CF direction. At a low reduced velocity, the gas curtain does not appear at the tail of the riser, which results in an unsatisfactory vibration suppression effect of the active vibration suppression device on the riser. As the reduced velocity increases, the position of the gas curtain begins to move gradually toward the tail of the riser. The peak value of the vibration suppression efficiency appears in the strong disturbed flow region in turn. This is because when the gas curtain enters the strong disturbed flow region, the blocking effect of the reverse circulation causes the amplitude of the riser in the IL direction to be greatly reduced. It is worth

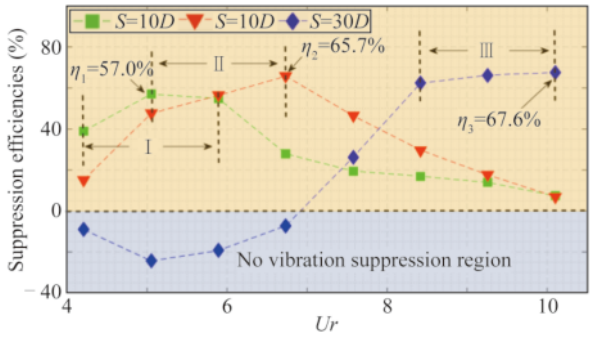

Fig. 11. Suppression efficiencies of the active jet vibration suppression device for CF riser vibration at different spacings.

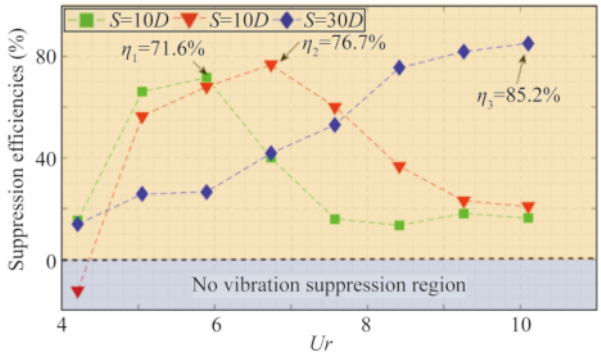

Fig. 12. Suppression efficiencies of the jet-type active vibration suppression device for IL riser vibration at different spacings.

noting that the vibration suppression efficiency of the active vibration suppression device in the IL direction of the riser in the strong disturbed flow region is much better than that in the CF direction.

3.4 CF and IL coupled vibration of the riser

Fig. 13 shows the displacement trajectories of the riser along the reduced velocity before excitation and after excitation at different spacings. From this figure, the displacement trajectories of the pre-excitation riser are a regular "8" and these figures enlarge continuously along the reduced velocity. Obviously, there is a strong nonlinear coupling between the CF and IL of the riser. When $5.05 \leqslant Ur \leqslant 6.73$, the displacement trajectories at both $S = 10D$ and $S = 15D$ show an obvious difference from their pre-excitation counterparts: their shapes change from a crescent or "8" to an "O", the displacement amplitude reduces significantly, and the circulation generated by the gas curtain destroys the strong nonlinear coupling in the two directions, as shown by the red shaded zone in the figure. Within this reduced velocity interval, at the excitation spacings of $S = 10D$ and $S = 15D$, the jet-type active vibration suppression device effectively prevent the formation of vortex shedding, thereby reducing the vibration amplitude of the riser. After this interval, as the reduced velocity increases, the displacement trajectories become an "8" again and the riser recovers its regular vibration, and the influence of the gas curtain on the vortex-induced vibration of the riser is gradually weakened, which is consistent with the phenomenon observed in Fig. 7. When $8.42 \leqslant Ur \leqslant 10.10$, the displacement trajectories at $S = 30D$ in the green shaded zone are even more different than their pre-excitation counterparts. The gas curtain is greatly influential to the vortex-induced vibration of the riser. The displacement trajectories change from an "8" to a smaller "O". It shows that the active vibration suppression device can effectively weaken the strong coupling effect of CF and IL in the strong disturbed flow region.

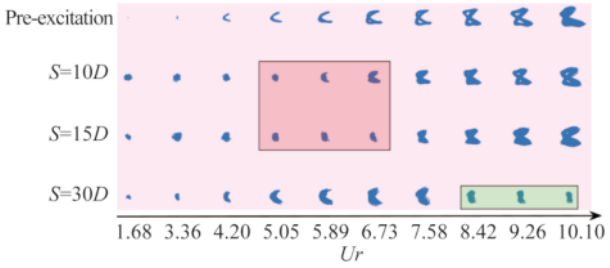

Fig. 13. Displacement trajectories of the jet-type active vibration suppression device along the reduced velocity before excitation and after excitation at different spacings.

4 Conclusions

In this paper, the jet-type active vibration suppression device and its test system have been designed to investigate the influence law of the jet-type active vibration suppression device on the dynamic response of the riser. The paper explores the disturbance suppression mechanism and sensitive characteristics of the jet-type active vibration suppression device, and the following conclusions can be drawn.

(1) After entering the strong disturbed flow region, the horizontally rising gas curtain flow has a significant influence on the dominant frequency of the riser at a low reduced velocity, and the vortex-induced vibration energy is attenuated by order of magnitude. When the gas curtain is in the weak disturbed flow region, the riser recovers the regular vortex-induced vibration, and the bubble injects momentum into the shear layer and the boundary layer, which extends the formation length of the vortex, and the dominant frequency decreases slightly.

(2) When the gas curtain is in the strong disturbed flow region, the reverse circulation formed by it hinders the formation and development of the boundary layer. Moreover, the rising gas curtain interrupts the wake of the riser, which effectively reduces the amplitude of the riser and stabilizes the amplitude at the same amplitude. In addition, the stable amplitude of the gas curtain in the strong disturbed flow region is weakly affected by the reduced velocity, and the jet-type active vibration suppression device has more advantages at high reduced velocity.

(3) Different excitation spacings cause the gas curtain to enter the strong disturbed flow region at different velocities

and inclination angles, and the peak value of the vibration suppression efficiency appearing in the region is also slightly different. The coupling relationship between the excitation spacing and the reduced velocity is the key factor for the gas curtain to enter the strong disturbed flow region, which can achieve the optimal disturbance suppression effect.

(4) The coupled vibration in the CF and IL directions of the pre-excitation riser gradually shows a shape of "8" with the increase of the reduced velocity, and the jet-type active vibration suppression device interferes with its strong nonlinear coupled vibration in the strong disturbed flow region. Obviously, in the entire strong disturbed flow region, the dimensionless displacement in both directions is greatly reduced, and the displacement trajectory is changed to "O" type. When the gas curtain enters the weak disturbed flow region, its displacement trajectory is transformed from "O" type to "Crescent" shape and then re-converts to "8" shape with the gradual increase of the reduced velocity, and the disturbance vibration suppression effect is gradually reduced.

References

Baarholm, G.S., Larsen, C.M. and Lie, H., 2006. On fatigue damage accumulation from in-line and cross-flow vortex-induced vibrations on risers, *Journal of Fluids and Structures*, 22(1), 109–127.

Chaplin, J.R., Bearman, P.W., Huera-Huarte, F.J. and Pattenden, R.J., 2005. Laboratory measurements of vortex-induced vibrations of a vertical tension riser in a stepped current, *Journal of Fluids and Structures*, 21(1), 3–24.

Cheng, L., Zhou, Y. and Zhang, M.M., 2003. Perturbed interaction between vortex shedding and induced vibration, *Journal of Fluids and Structures*, 17(7), 887–901.

Cicolin, M.M. and Assi, G.R.S., 2017. Experiments with flexible shrouds to reduce the vortex-induced vibration of a cylinder with low mass and damping, *Applied Ocean Research*, 65, 290–301.

Dong, S., Triantafyllou, G.S. and Karniadakis, G.E., 2008. Elimination of vortex streets in bluff-body flows, *Physical Review Letters*, 100(20), 204501.

Feng, L.H. and Wang, J.J., 2014. Modification of a circular cylinder wake with synthetic jet: Vortex shedding modes and mechanism, *European Journal of Mechanics - B/Fluids*, 43, 14–32.

Gao, Y., Fu, S.X., Yang, J. D. and Wang, M.H., 2016. Fatigue damage analysis of vortex-induced vibration of a long flexible riser, *Journal of Shanghai Jiaotong University*, 50(8), 1270–1277. (in Chinese)

Gao, Y., Wang, X.M., Xiong, Y.M., Zou, Z. and Zong, Z., 2017. Dynamic response and fatigue damage analysis of a steel catenary riser at the touchdown point considering seabed contact, *Chinese Journal of Computational Mechanics*, 34(6), 704–711. (in Chinese)

Huera-Huarte, F.J., 2014. On splitter plate coverage for suppression of vortex-induced vibrations of flexible cylinders, *Applied Ocean Research*, 48, 244–249.

Liu, S.Y., 2010. *Wave Dissipating Mechanism Study on Air Bubbles Breakwater*, MSc. Thesis, Dalian University of Technology, Dalian. (in Chinese)

Muddada, S. and Patnaik, B.S.V., 2010. An active flow control strategy for the suppression of vortex structures behind a circular cylinder, *European Journal of Mechanics-B/Fluids*, 29(2), 93–104.

Muddada, S. and Patnaik, B.S.V., 2017. Active flow control of vortex induced vibrations of a circular cylinder subjected to non-harmonic forcing, *Ocean Engineering*, 142, 62–77.

Song, L.J., Fu, S.X., Cao, J., Ma, L.X. and Wu, J.Q., 2016. An investigation into the hydrodynamics of a flexible riser undergoing vortex-induced vibration, *Journal of Fluids and Structures*, 63, 325–350.

Trim, A.D., Braaten, H., Lie, H. and Tognarelli, M.A., 2005. Experimental investigation of vortex-induced vibration of long marine risers, *Journal of Fluids and Structures*, 21(3), 335–361.

Wang, C.L., Tang, H., Yu. S.C.M. and Duan, F., 2017. Control of vortex-induced vibration using a pair of synthetic jets: Influence of active lock-on, *Physics of Fluids*, 29(8), 083602.

Wang, K.P., Tang, W.Y. and Xue, H.X., 2014. Cross-flow VIV-induced fatigue damage of deepwater steel catenary riser at touchdown point, *China Ocean Engineering*, 28(1), 81–93.

Wang, K.P., Xue, H.X. and Tang, W.Y., 2013. In-line VIV response and fatigue damage of a deepwater riser in linearly sheared flow, *Journal of Vibration and Shock*, 32(19), 1–6, 27. (in Chinese)

Warui, H.M. and Fujisawa, N., 1996. Feedback control of vortex shedding from a circular cylinder by cross-flow cylinder oscillations, *Experiments in Fluids*, 21(1), 49–56.

Williams, D.R., Mansy, H. and Amato, C., 1992. The response and symmetry properties of a cylinder wake subjected to localized surface excitation, *Journal of Fluid Mechanics*, 234, 71–96.

Williams, J.E.F. and Zhao, B.C., 1992. Active control of vortex shedding, *Journal of Fluids and Structures*, 3(2), 115–122.

Zhu, H.J., Tang, T., Zhao, H.L. and Gao, Y., 2019. Control of vortex-induced vibration of a circular cylinder using a pair of air jets at low Reynolds number, *Physical of Fluid*, 31(4), 043603.